Electronic Supplementary Material (ESI) for Journal of Materials Chemistry A.

Supporting Information

Simultaneous Enhancement in Performance and UV-light Stability for Organic-Inorganic Perovskite Solar Cells Using Samarium-based Down Conversion Material

Naveed Ur Rahman, Wasim Ullah Khan, Wenlang Li, Shaukat Khan, Javid Khan, Shizhao Zheng, Tongtong Su, Juan Zhao *, Matthew P. Aldred, Zhenguo Chi**

1. Device fabrication and characterization

The patterned Fluorine-doped tin oxide (FTO) substrates with a sheet resistance of 7 Ω/sq were sequentially cleaned by sonication with acetone, detergent, deionized water and isopropyl alcohol for 15 min respectively, followed by oxygen plasma treatment to remove organic impurities. Then, a compact TiO_2 (c-TiO_2) layer was deposited on the pre-treated FTO substrates by spray pyrolysis from a precursor solution of titanium diisopropoxide bis (acetylacetonate) solution, and annealed at 500 °C for 50 min. The SCOS layer was prepared by spin coating on c-TiO_2 at 5000 rpm for 20 s and annealed at 450 °C for 30 min. For one-step method, PbI_2, FAI, MABr, and $PbBr_2$ were dissolved together in a mixed solvent of DMF and DMSO (DMF: DMSO = 4:1 in volume ratio) to form a 1 M precursor solution. The MABr and $PbBr_2$ (1:1 molar ratio) had 10 mol% in total perovskite precursor solution. In one-step method, a 45 μL of mixed perovskite precursor solution was first dropped on the SCOS layer and then the spin coating was started. The spin rate was 1000 rpm for 10 s in the step one and then increased to 6000 rpm for 20 s in the step two. 100 μL of chlorobenzene was dropped onto the spinning film 5 s prior to the end of the second step. The as-prepared films were then dried at 70 °C for 10 min and thermally annealed at 100 °C for 90 min. All the film deposition processes were performed in an N_2-filled glove box. Spiro-OMeTAD was used as the HTM layer on the mixed cation perovskite layer by spin-coating of a 45 μL prepared solution 85.7 mg, 33.84 μL 4-tert-butylpyridine, 10.05 mg lithium bis (trifluoromethyl sulphonyl) imide and 3.16 mg FK209 dissolved in 1 mL chlorobenzene) at 4000 rpm for 20 s. Finally, Au back electrode with a thickness of 100 nm was thermally evaporated on the HTM layer. The photocurrent density–voltage (*J*–*V*) curve were measured using a solar simulator with Keithely model 2400 as a digital source meter under the illumination of the simulated 100 mW cm^{-2}AM 1.5G solar light (ABET Sun 3000 solar simulator). The active area of the solar cells was defined as 0.07 cm^2 by using a metal mask. During the photovoltaic performance characterization, the applied bias voltages for the reverse and forward scan were from 1.2 to 0 V and 0 to 1.2 V with a scan rate of 30 mV s^{-1}. The incident photon to current efficiency (IPCE) as a function of wavelength of the PSCs was measured by a PV measurements QEXL from 300 nm to 900 nm. The devices were tested in ambient environment at 25 ^{o}C and 30 – 50% relative humidity (RH). Electrochemical impedance spectroscopy (EIS) of the devices were performed by BioLogic Science Instruments VMP-300 multipotentiostat. The EIS results were measured over a frequency range of 0.1 – 100 kHz, and the applied bias voltage was set as 0.8 V.

2. Supplementary tables and figures

Table S1. Percent surface elemental composition of $Sr_2CeO_4:Sm^{3+}$ calculated from the XPS results.

Element	**composition [%]**
Oxgen	75.44
Strontium	24.47
Cerium	0.06
Samarium	0.03

Table S2. Performance comparison of perovskite solar cells based on various down conversion phosphor materials.

Materials	**J_{sc} [mA cm^{-2}]**	**V_{oc} [V]**	**FF [%]**	**PCE [%]**	**UV stability[a]**	**Ref.**
$Sr_2CeO_4:Sm^{3+}$	23.65	1.05	72.4	17.9	50%, 60 h	This work
$CeO_2:Eu^{3+}$	20.50	0.90	58.7	10.8	68%, 0.8 h	[1]
$ZnGa_2O_4:Eu^{3+}$	25.68	0.94	62.6	14.3	Not given	[2]
Eu-complex	19.60	1.05	75.9	15.4	50%, 10 h	[3]
$SrAl_2O_4:Eu^{2+}$, Dy^{3+}	21.70	1.09	75.8	17.8	92%, 100 h	[4]
$Au@Y_2O_3:Eu^{3+}$	21.50	1.02	73.5	16.1	40%, 24 h	[5]

[a] UV stability: how much PCE remains in percent compare to the initial value after a specific time period.

Table S3. Fitting results from R_s ($C_{rec}R_{rec}$) equivalent circuit. The active area of the samples was 0.16 cm^2.

Device	**Bias [V]**	**R_s [Ω]**	**R_{rec} [Ω]**
SCOS	0	7.37E+001	5.24E+003
Control	0	8.62E+001	4.36E+003
SCOS	0.8	9.55E+001	1.03E+003
Control	0.8	10.55E+001	0.87E+003

Table S4. The performance of PSCs with different thicknesses for the SCOS layer.

Cell architecture	Thickness of SCOS [nm]	J_{sc} [mA cm^{-2}]	V_{oc} [V]	FF [%]	PCE [%]
FTO/c-TiO$_2$/SCOS/ Perovskite/HTM/Au	120	20.75	1.02	70.9	15.0
As above	150	23.65	1.05	72.4	17.9
As above	170	19.83	0.99	70.2	14.0

Table S5. PCEs for nine cells of the SCOS device and control device as a function of UV-light radiation hours.

Cell No.	Condition	PCE [%]			
		Initial	After 15 h	After 30 h	After 60 h
1	SCOS devices @ ambient condition	17.1	13.4	12.1	11.1
2		17.7	13.6	12.3	11.0
3		16.4	13.3	12.1	11.2
4		15.8	13.7	12.5	11.5
5		16.5	13.2	11.9	11.4
6		15.9	12.9	11.7	10.9
7		17.0	13.5	12.4	11.1
8		16.7	13.0	11.8	11.2
9		16.0	12.8	11.7	10.6
1	Control devices @ ambient condition	15.0	7.2	4.6	-
2		15.5	7.4	4.5	-
3		15.2	7.0	4.3	-
4		14.8	6.7	4.2	-
5		14.5	6.4	3.8	-
6		14.3	6.1	3.7	-
7		14.9	6.8	4.9	-
8		15.1	7.3	4.6	-
9		14.7	6.6	4.0	-

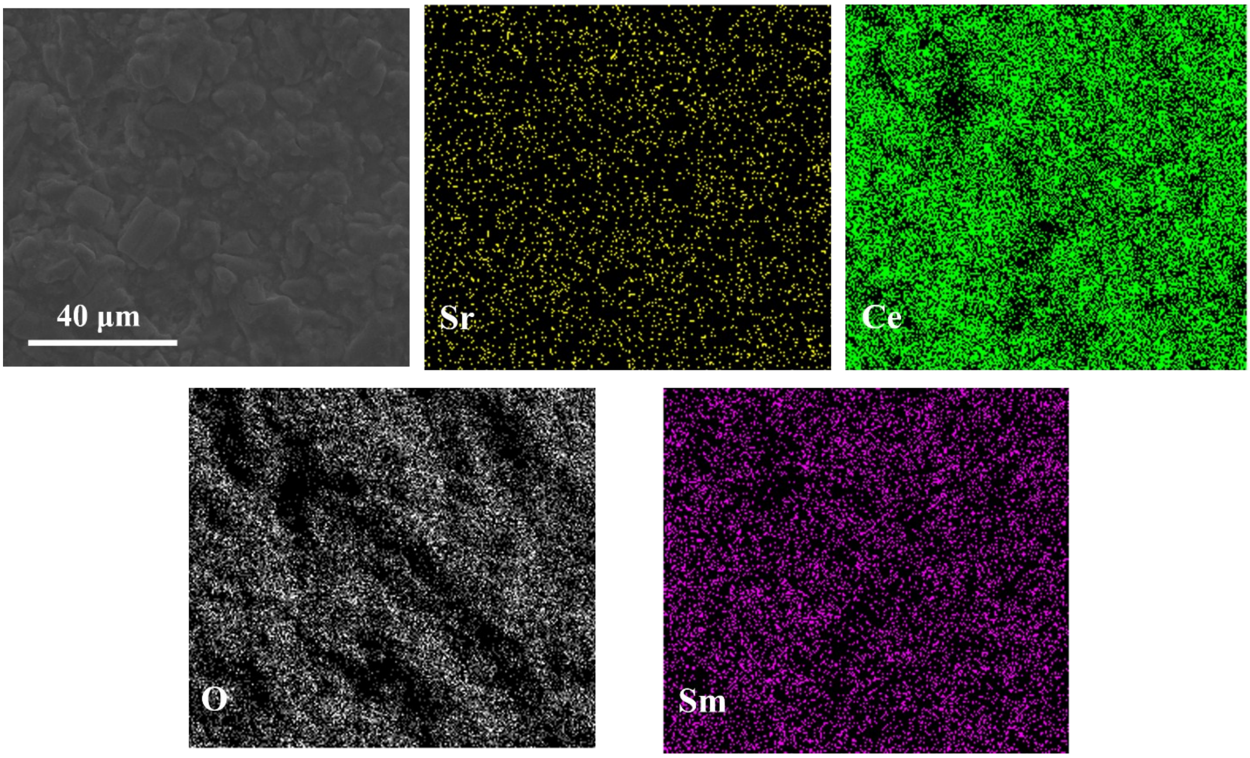

Figure S1. EDS mapping of SCOS pellet confirms the presence and uniform distribution of Sr, Ce, O and Sm elements in the materials and also successful doping with Sm.

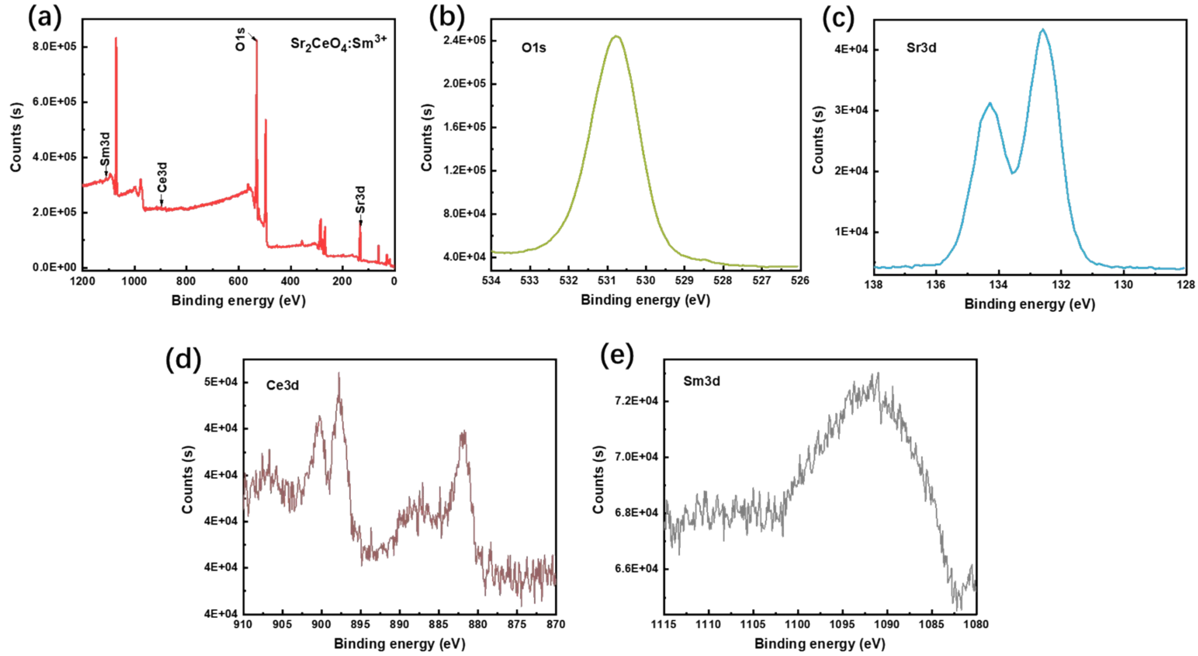

Figure S2. XPS spectra of (a) $Sr_2CeO_4:Sm^{3+}$, (b) O1s, (c) Sr3d, (d) Ce3d and (e) Sm3d core levels. The peak at 530.7 eV is identified to be O1s peak, the Sr $3d_{5/2}$ and $3d_{3/2}$ peaks are observed at 132.6 eV and 134.3 eV respectively, Ce $3d_{5/2}$ and $3d_{3/2}$ peaks appear at 881.8 eV and 900.2 eV respectively, Sm $3d_{5/2}$ and $3d_{3/2}$ peaks are assumed to be 1083.8 eV and 1110.4 eV respectively.[6]

Solvent selection was initially performed to optimize better dispersion and stable suspension for thin layer formation. The SCOS material was suspended in tested solvents through ultrasonication for 30 min. The experiment was repeated systematically and pictures of the suspensions were taken at various time intervals to show their stability in the tested solvents. As evident from Figure S4, 2-Methoxyethanol was chosen as a solvent of choice for thin layer fabrication due to its ability to form uniform and stable suspension of the nanophosphors. The solution was 5 mg/ml, which is sonicated for 1 hour. The stability of the SCOS solution with time interval is shown in Figure S2.

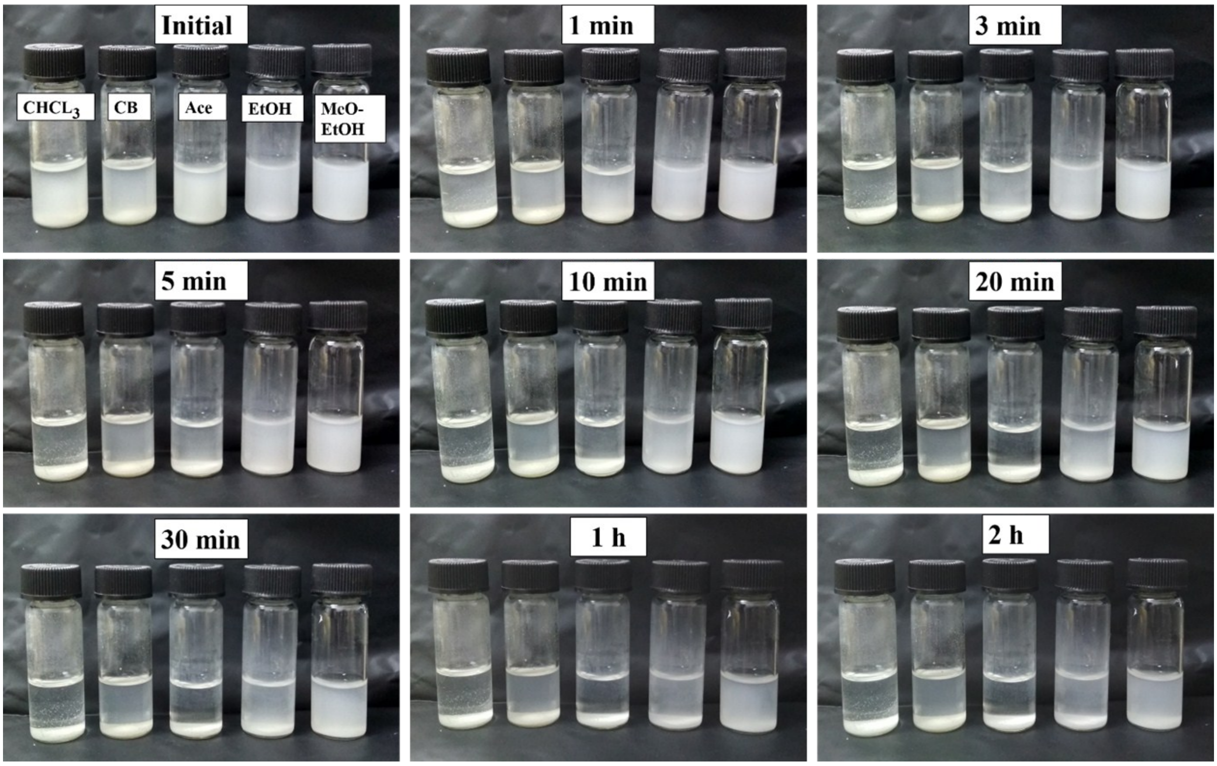

Figure S3. SCOS based suspension stability in different solvent with respect to time interval. The solvents names were only added to the first picture while the rest of the pictures show the suspensions in the same order.

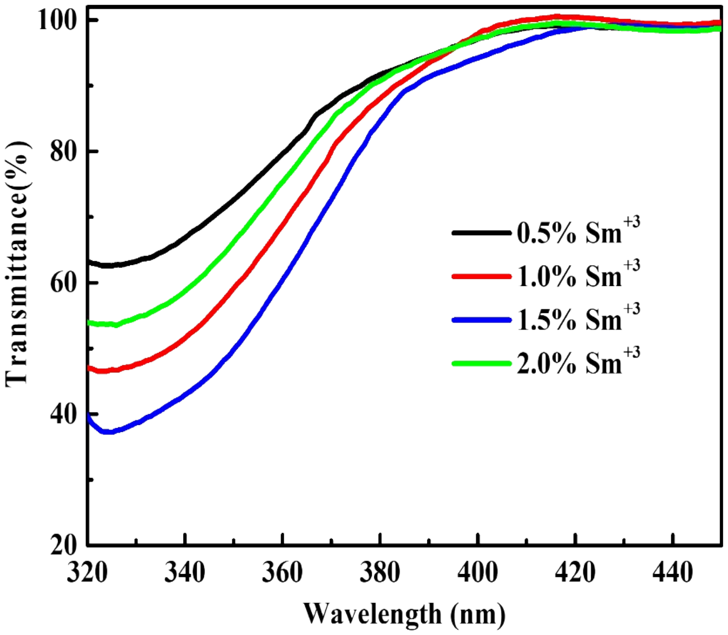

Figure S4. Transmission spectra of the SCOS films with different Sm^{3+} doping concentrations in the UV region.

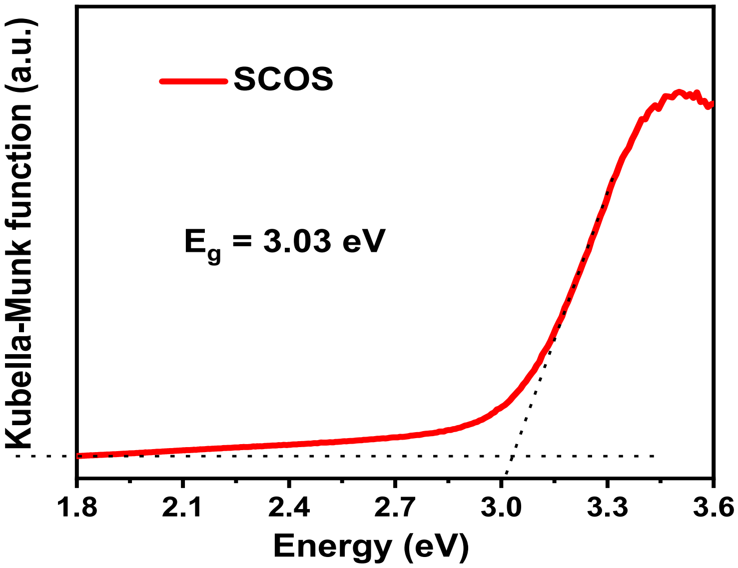

Figure S5. Diffused reflectance spectrum (DRS) of the SCOS nanoparticles. The energy band gap (E_g) was calculated to be 3.03 eV, which was determined from the intersection point between the energy axis at the absorption offset and the line extrapolated from the sharp absorption edge.

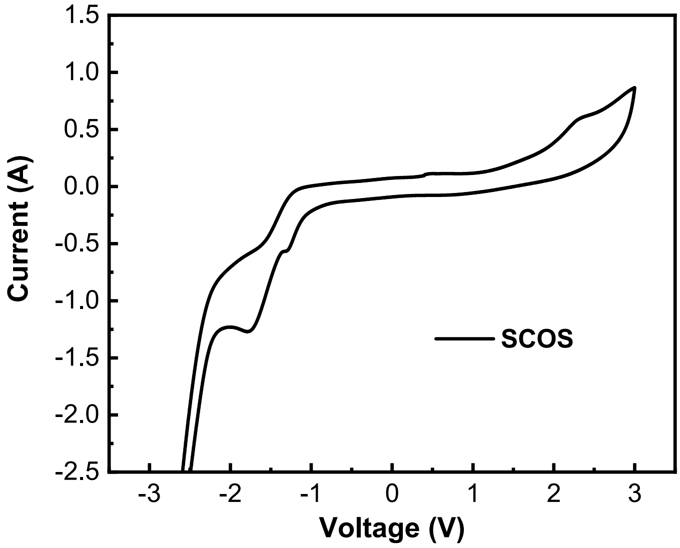

Figure S6. The cyclic voltammetry characteristic of the SCOS nanoparticles. HOMO is deteimied by HOMO = −4.8 − (E_{ox}−$E_{1/2(Ferrocene)}$),[7] where E_{ox} is the oxidation potential point, $E_{1/2(Ferrocene)}$ is the oxidation potential of ferrocene (F_c/F_c^+) and measured to be 0.18 eV.

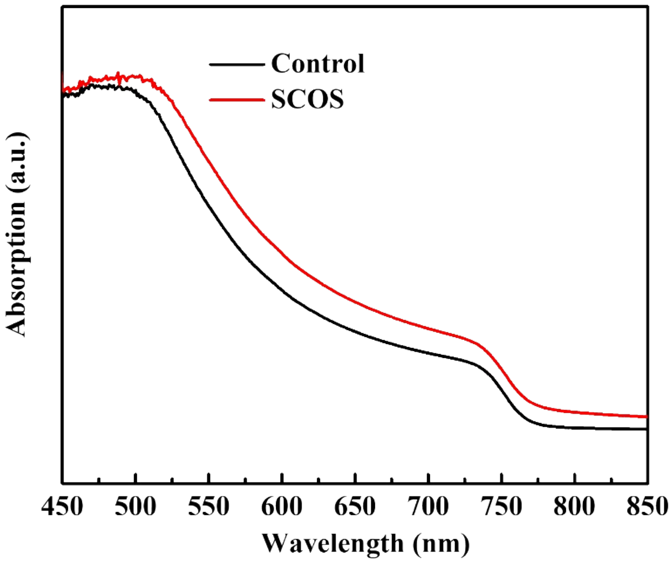

Figure S7. UV-vis absorption spectra of two samples including FTO/c-TiO_2/SCOS/ perovskite (SCOS sample) and FTO/c-TiO_2/perovskite (control sample).

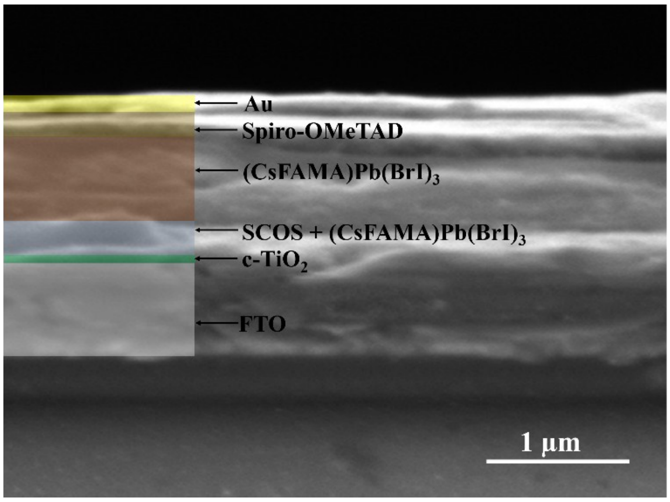

Figure S8. Cross sectional SEM of the SCOS-based PSCs.

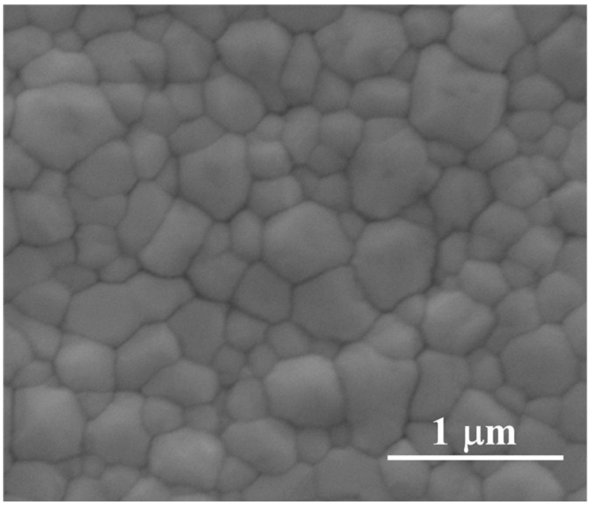

Figure S9. SEM image of (CsFAMA)Pb(BrI)$_3$ film coated on c-TiO$_2$/SCOS.

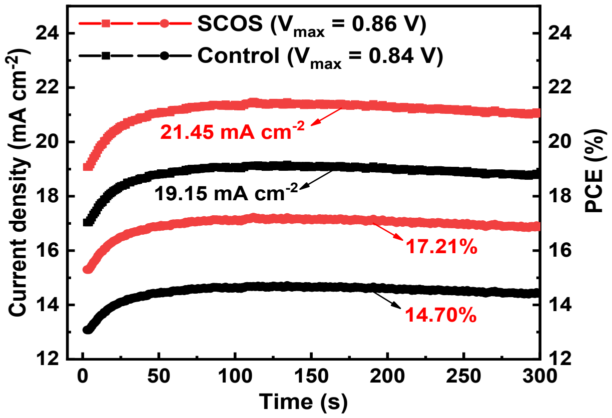

Figure S10. Steady-state current density and PCE as a function of time for the control and SCOS-based devices.

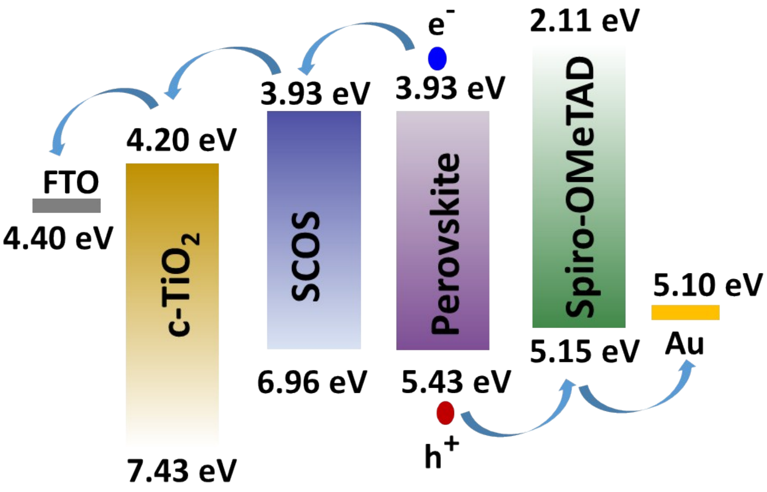

Figure S11. Energy band alignment of the samarium-based perovskite solar cells.

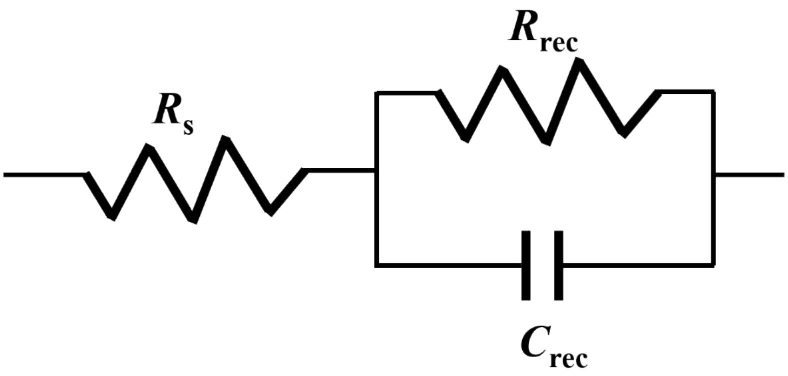

Figure S12. R_s ($C_{rec}R_{rec}$) equivalent circuit utilized to fit the Nyquist plots of PSCs.

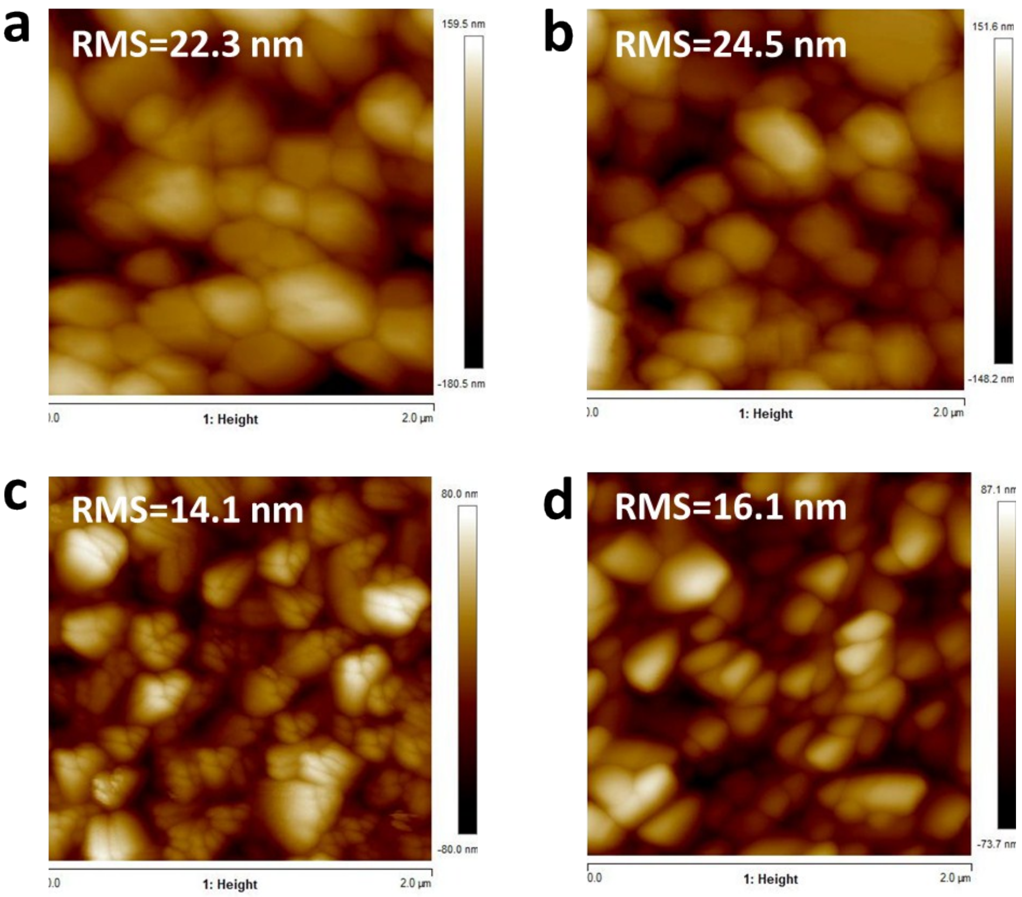

Figure S13. AFM images of a perovskite film coated on (a) SCOS film and (b) TiO_2 film. AFM images of (c) a SCOS film and (d) a TiO_2 film.

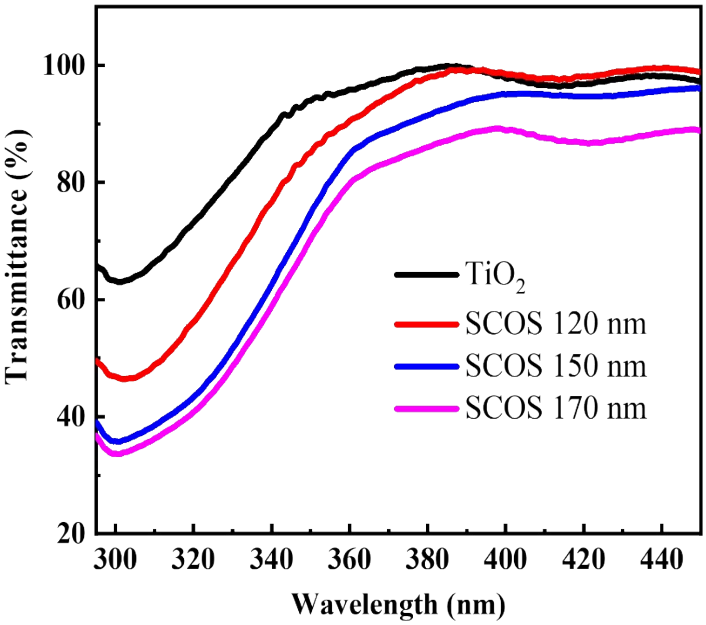

Figure S14. Transmission spectra of FTO/c-TiO_2 sample and FTO/c-TiO_2/SCOS (120, 150, and 170 nm) samples.

References

[1] W. Chen, Q. Luo, C. Zhang, J. Shi, X. Deng, L. Yue, Z. Wang, X. Chen, S. Huang, *J. Mater. Sci.: Mater. Electron.* **2017**, *28*, 11346.

[2] X. Hou, T. Xuan, H. Sun, X. Chen, H. Li, L. Pan, *Sol. Energ. Mater. Sol. Cells* **2016**, *149*, 121.

[3] L. Jiang, W. Chen, J. Zheng, L. Zhu, L. Mo, Z. Li, L. Hu, T. Hayat, A. Alsaedi, C. Zhang, *ACS Appl. Mater. Interfaces* **2017**, *9*, 26958.

[4] C. Chen, H. Li, J. Jin, X. Chen, Y. Cheng, Y. Zheng, D. Liu, L. Xu, H. Song, Q. Dai, *Adv. Energ. Mater.* **2017**, *7*, 1700758.

[5] C. W. Kim, T. Y. Eom, I. S. Yang, B. S. Kim, W. I. Lee, Y. S. Kang, Y. S. Kang, *Sci. Rep.* **2017**, *7*, 6849.

[6] http://www.xpsdata.com/.

[7] Q. Li, Y. Yuan, T. Wei, Y. Li, Z. Chen, X. Jin, Y. Qin, W. Sun, *Sol. Energ. Mater. Sol. Cells* **2014**, 130, 426.